

Performance Parameters of Graphite and Platinum Counter electrode Based Dye Sensitized Solar Cells

Amrik Singh^{1*}, Dharamvir S. Ahlawat¹, Devendra Mohan²,
Divya J. Chawla³ and Richa⁴

¹Material Science Laboratory, Department of Physics, Chaudhary Devi Lal University,
Sirsa-125055 Haryana (India)

²Laser Laboratory, Department of Applied Physics,
Guru Jambheshwar University of Science & Technology, Hisar-125001, Haryana (India)

³Department of Physics, University College, Jaitu, Punjab (India)

⁴Department of Physics, I. K. Gujral Punjab Technical University,
Kapurthala, Punjab (India)

*E-mail: amrik23kuk@gmail.com

(Received 27 February 2018, Accepted 23 March 2018, Published 04 May 2018)

Abstract

In the present course of work, we have successfully prepared a dye sensitized solar cell (DSSC) based on TiO₂ film coated ITO (indium doped tin oxide) glass photo anode, N719 dye as sensitizer, iodine as redox couple electrolytes and a counter electrode with graphite film coated ITO glass. Powder of TiO₂ was synthesized by sol gel route technique. The XRD pattern confirms the anatase and rutile phase of TiO₂. Crystallite size of TiO₂ powder is 75.5nm. The TiO₂ paste was coated on ITO by doctor blade technique. The FTIR spectrum shows a main peak corresponding to 495cm⁻¹. However, UV-Visible absorbance of graphite/ITO glass and platinum/ITO glass were obtained as 20-25% and 7-17% respectively in the wavelength range of 300-800nm. The open circuit voltage of DSSC has been observed to be maximum 690.1mV and 619.5mV for platinum and graphite counter electrode respectively. The OCV decay shows the non linear nature. The fill factor values were obtained as 0.60 and 0.50 for platinum and graphite based electrode of DSSCs respectively. The efficiencies of DSSC with platinum/ITO and graphite/ITO electrodes were found to be 1.63% and 0.89% respectively.

Keywords: TiO₂ powder, solar cell preparation, performance of DSSCs

1. Introduction

Photovoltaic (PV) energy is known to be a cleanest and largest energy source all over the world. But due to the high cost of conventional solar cells, which are mainly based on Si, PV electricity has not been utilized on a large scale for power production. However, Dye sensitized solar cells

(DSSC) have attracted a great attention due to their low cost, easy fabrication and stability [1-3]. These dye sensitized solar cells have a photo-anode and counter-electrode with electrolytes sandwiched between the electrodes.

The photo-anode consists of dye adsorbed semiconductor oxide layer like ZnO, TiO₂ coated on TCO (transparent conducting oxide) glass substrate and counter-electrode have platinum/graphite coated film on TCO glass substrate like ITO (Indium doped tin oxide), FTO (Flourine doped tin oxide). Iodine electrolytes act as redox couple in which oxidation and reduction occur. As sunlight fall on the dye adsorbed semiconductor oxide layer, dye molecules absorb the photons and consequently the electrons of semiconductor oxide film gets excited. The electron reach to outer path via TCO, at another end counter-electrode collects the electrons that oxidizes the iodine.

The TiO₂ materials are wide band gap semiconductor with some important applications like in anti reflective coating, solar cells etc. Its properties like excellent optical transmittance, high refractive index, inertness to chemical environment and long term photo-stability make this material a good candidate for AR coating and solar cells [4-7]. The performance of TiO₂ has been found to be excellent as compared to other types of oxides in solar cells [8].

There are many techniques for film coating like sol-gel dip, spin coating, spray pyrolysis, doctor blade technique etc. In the present work, we have employed the doctor blade technique to coat the TiO₂ film on ITO substrate. The main merits of this method are that it is economical and produces a uniform film in a short time [9-15]. The influence of counter electrode materials on the performance of DSSC has been investigated. Moreover we have also studied the performance of DSSC with different counter electrodes. The XRD, SEM and FTIR analysis of TiO₂ films have been obtained.

The counter electrode material plays an important role in altering the performance of DSSC. The role of counter electrodes is to transfer electrons from the external circuit to the tri-iodide and iodine in the redox electrolyte [16]. This research paper reports the fabrication and characterization results of platinum and graphite counter electrodes based dye sensitized solar cells. Graphite provides a promising alternative to platinum owing to their intrinsic attractive features as well as their increasingly affordable cost.

2. Experimental Detail

2.1 Materials used

Titanium Isopropoxide (TTIP, Sigma Aldrich > 97%), Ethanol (Merck, 99% USA), Lithium Iodide (Sigma Aldrich, 99.9%), Iodine (Sigma Aldrich, 99.9%), Acetonitrile (Sigma Aldrich 99.9%), Platinum Tetrachloride (Sigma Aldrich, 99.9%), Isopropanol (Sigma Aldrich, 3050 Spruce Street, Saint Louis, MO 63103, USA,)

2.2 Preparation of TiO₂ paste

TiO₂ powder was prepared by taking Titanium Isopropoxide (TTIP, Sigma Aldrich > 97%), distilled water and ethanol (Merck) as the starting precursors. First, the TTIP was added to the ethanol to form a solution A. Then the stirring speed was adjusted to 500 rpm. Now the acetic acid was added into the distilled water to form a solution B. After that the solution B was added to

solution A. After four hours of continuous stirring the solution was putted on room temperature (31°C- 37°C) for 12 hours. After that the solution was kept at 100°C for 12 hours and the obtained product is a dry powder. Now wash the powder with filter paper many times so as to remove the impurities and again dry to remove the distilled water.

The dry TiO₂ powder was grounded with a pestle mortar for 2 hours. Heat the synthesized powder at 450°C with a temperature gradient 10°C/minute for one hour. For preparation of TiO₂ film, binder were prepared by the following steps first ethylene glycol, Titanium isopropoxide (TTIP) and citric acid were mixed to form solution A. The molar ratio of ethylene glycol, citric acid and TTIP is taken as 24:7:1. TiO₂ powder were mixed solution A in pestle mortar to form TiO₂ paste [17]. However, ITO glasses were used as substrate material for photo-anode and counter-electrode. The film prepared with this binder is highly adhesive in nature with ITO glass substrate. The components of DSSC are shown in figure 1.

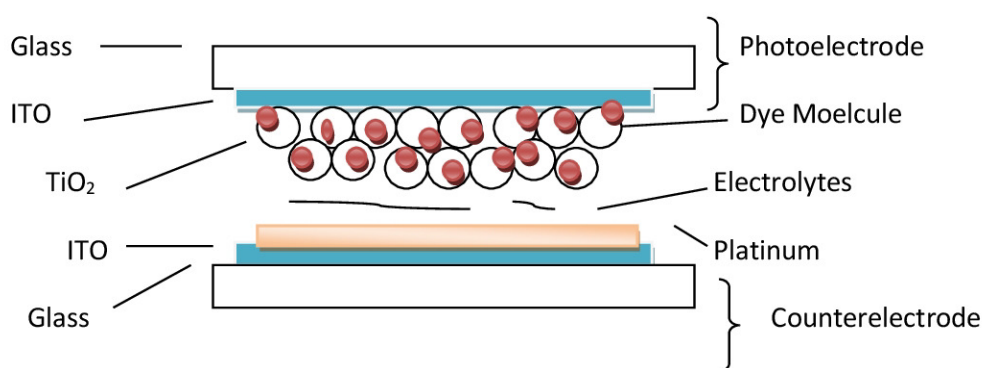


Figure1 : Structure of DSSC

2.3 Preparation of photo-electrode of DSSC

Indium doped tin transparent conducting oxide (TCO) acts as a substrate for both photo-electrode and counter-electrode of the dye-sensitized solar cell. The substrate was first dipped into acetone with ultrasonic bath for 10 minutes to dissolve unwanted organic materials so that contamination material was removed which was left on the substrates during preparation. Another 10 minutes of ultrasonic bath in ethanol was followed in order to remove the acetone and materials that were not cleansed or dissolved by acetone. Finally, a 10 minutes ultrasonic bath in isopropanol was also needed to further remove the residual particles on the substrates.

The TiO₂ paste was coated onto an ITO glass substrate using a doctor blade technique and annealed at 450°C for one hour. After annealing the cooled film were immersed in a 5mM ethanolic N719 solution for 24 hrs, and the dye adsorbed films were rinsed with absolute ethanol. For counter-electrode a graphite film was coated on another ITO glass substrate and for preparation of platinum film, 5 mM PtCl₄ and Isopropanol were mixed to make platinum solution. Pt film was coated on ITO/Glass by spin coater (MTI corporation) and then heated at 130°C for 10 minutes. After this, film has been annealed at 450°C with 10°C/minute for 15minutes.

The sensitized TiO₂ photo-anode and the counter electrode were stacked together face to face. Further the Iodine electrolytes solution was also prepared from Lithium Iodide and Iodine in

acetonitrile. The drops of prepared electrolyte solution drop penetrated into the space between photo-electrode and counter electrode [18]. The two electrodes were held together with clips as shown in figure 1.

2.4 Characterization Techniques

Structural properties were measured by the XRD set up type model (Panalytical's X'Pert Pro) The SEM measurement were taken on (SEM, JEOL). The FTIR (Perkin Elmer - Spectrum RX-IFTIR) spectra were recorded to measure the optical properties of the samples. The Hitachi 330 Model was used to record the UV-Visible Spectra of prepared samples. The photocurrent-voltage (J-V) measurements were also performed by using Solar Simulator (Xenon Lamp, 150W, AM 1.5) at room temperature. The active area of the sample is taken 1cmx1cm.

3. Results and Discussions

3.1 XRD

The XRD patterns of TiO₂ powder and TiO₂ film have been taken in the angle range from 20°-60° as shown in the figure 2 and 3 respectively. The XRD of TiO₂ powder demonstrated the planes (101), (110), (101), (103), (004), (112), (200), (105) and (211) at angle 25.92°, 27.83°, 36.50°, 37.40°, 37.98°, 38.98°, 48.59°, 54.64°, 55.79° respectively. The peaks at angles 25.92(101), 37.40(103), 37.98(004), 38.98(112), 48.59(200), 54.64(105), 55.79(211) and 27.83(110), 36.50(101) corresponding to anatase and rutile phase respectively. The XRD peaks of TiO₂ film were at angles 25.32°, 27.53°, 36.10°, 37.10°, 37.95°, 38.68°, 48.19°, 54.14°, 55.19° corresponding to planes (101), (110), (101), (103), (004), (112), (200), (105) and (211) respectively. The TiO₂ film was observed to be anatase and rutile phase. The Scherrer's equation (1) was used to calculate crystallite size, where k is the shape factor, λ is the x-ray wavelength, β is the line broadening at half the maximum intensity (FWHM) in radians, and θ is the Bragg angle, D is the mean size of the ordered (crystalline) domains, which may be smaller or equal to the grain size [19-21].

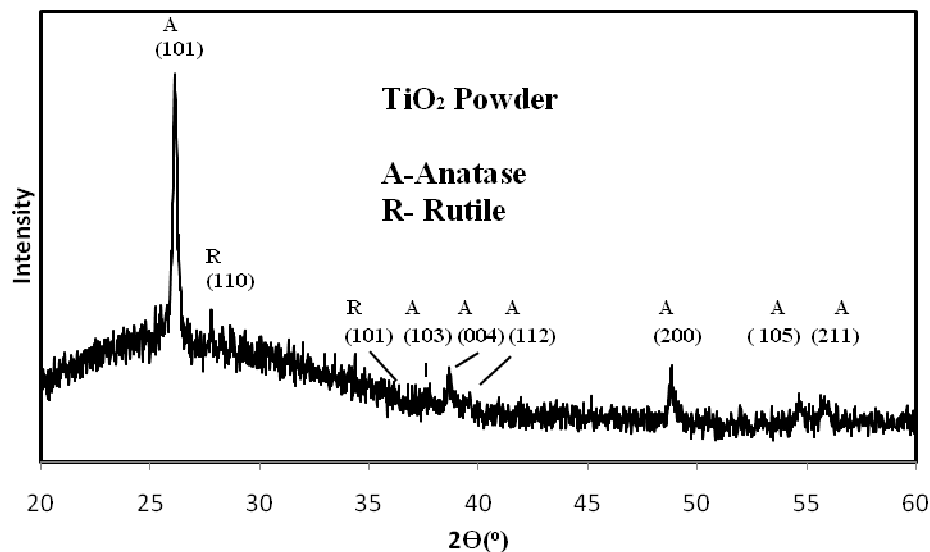


Figure 2 XRD pattern of TiO₂ powder.

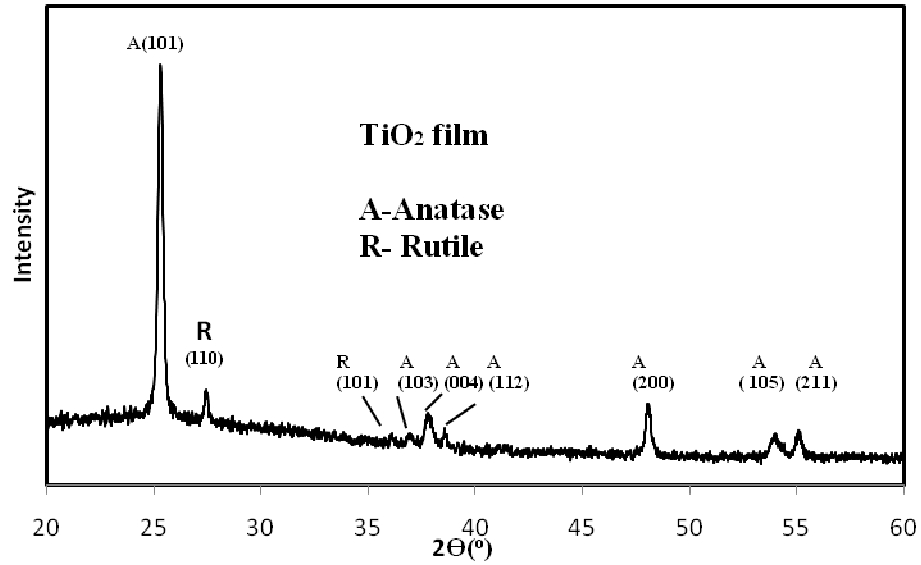


Figure 3 XRD pattern of TiO₂ film.

$$D = \frac{K\lambda}{\beta \cos\theta} \quad (1)$$

The crystallite size of TiO₂ powder and film are 75.5nm and 68.5nm respectively

3.2 SEM image of TiO₂ film

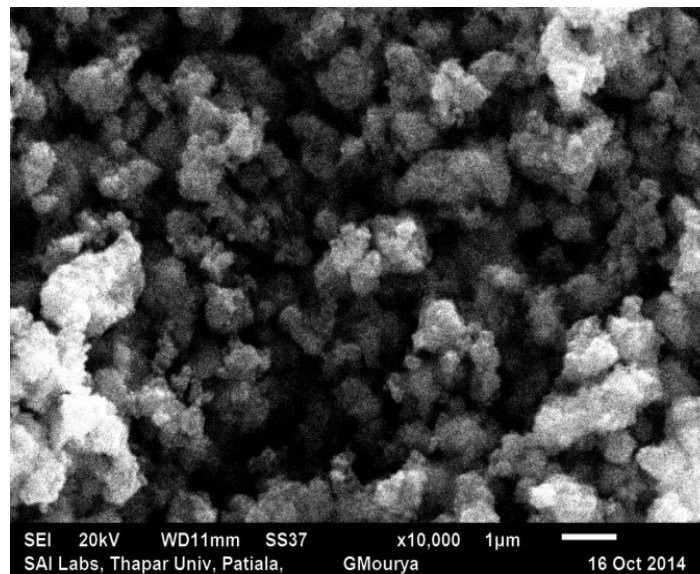


Figure 4 SEM image of TiO₂ Powder.

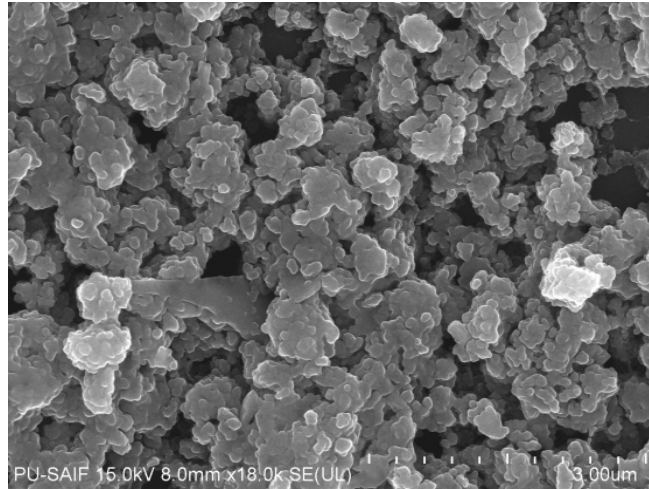


Figure 5 FE-SEM image of TiO₂ film.

Figure 4 demonstrates the SEM image of TiO₂ powder heated at 450°C. The grain of the TiO₂ powder aggregate to form clusters. Furthermore field emission scanning electron microscopy (FE-SEM) was also used to investigate the morphology shown in the fig.5. The SEM results of showed a rough morphology. FESEM image in fig. 5 show that film is porous in nature. The grain size calculated from figure5 was found to be 50.4nm. The grains are irregular in shape.

3.3 EDX

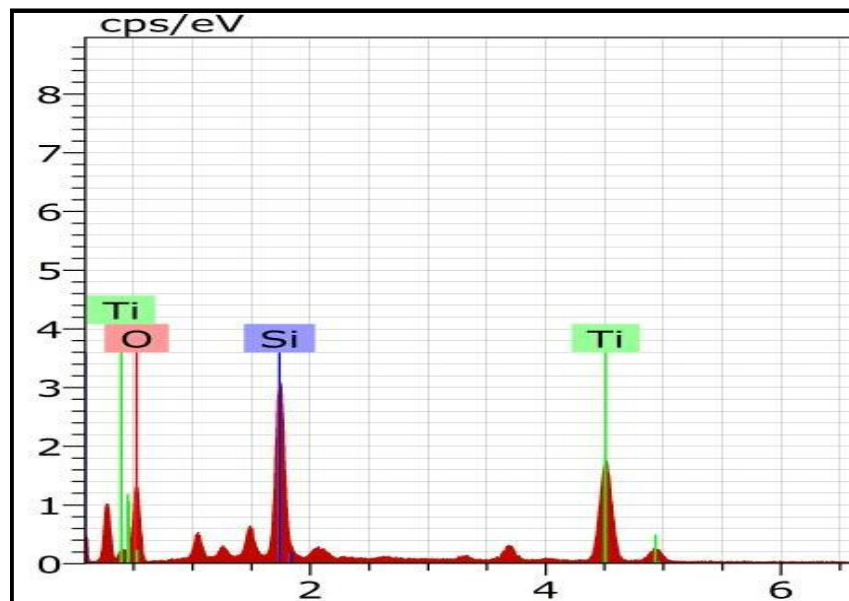


Figure 6 EDX spectra of TiO₂ film.

In energy dispersive spectroscopy, the EDX spectra of TiO₂ film is shown in Figure 6. The chemical compositions of TiO₂ from fig.7 showed the characteristic X-ray energy level of titanium, oxygen and other elements. The peak corresponding to Silicon is due to glass that acts as a substrate. The weight percentage of titanium, oxygen and silicon are 45.15% and 35.15% 18.16% respectively.

3.4 FTIR

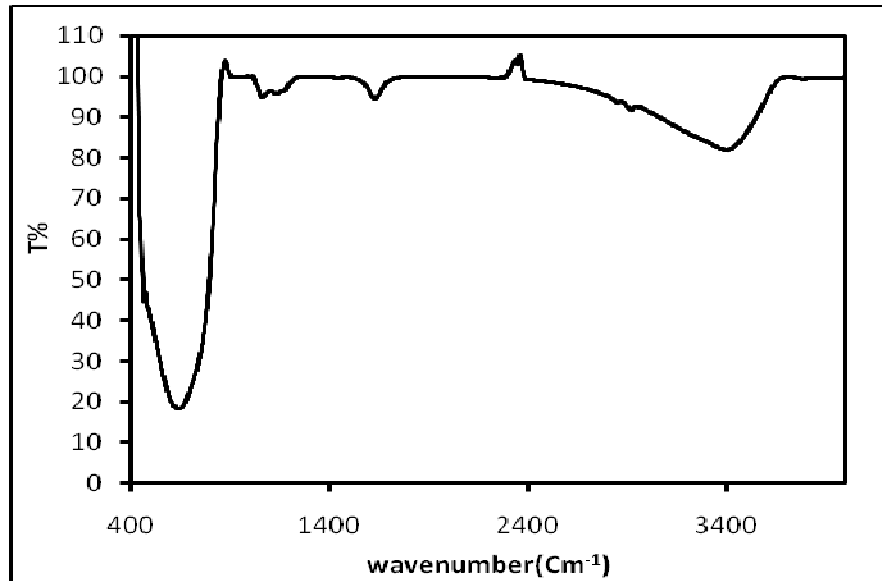


Figure 7 FTIR of TiO₂ powder

In order to understand the nature of residual in the samples, the FTIR spectra of thermally treated powder was also recorded as shown in the figure7. The as synthesized sample shows the characteristic absorptions peaks with a strong absorption at around 495cm⁻¹ and weak absorption in the range 510-3400 cm⁻¹. It can be observed apparently that a strong band in the range of 495 to 660 cm⁻¹ is associated with the characteristic modes of TiO₂. However, there is an OH stretch (2800-3600 cm⁻¹) and a Ti-O stretch (400-1000 cm⁻¹). The absorption range around 3400cm⁻¹ indicates that the presence of hydroxyl group. The absorption range around 1630 cm⁻¹ may be related to hydroxyl groups of molecular water [22].

3.5 UV-Visible Absorbance

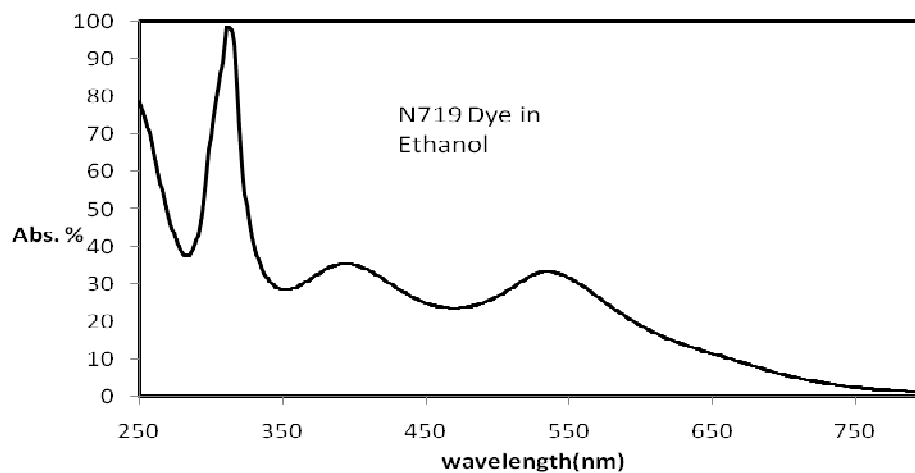


Figure 8 UV-Visible spectrum of N719 dye ethanol solution.

Figure 8 demonstrates the UV- visible spectrum of N79 dye ethanol solution in the wavelength range 250-800nm. The main absorption peaks lie at 305nm, 395nm and 545nm. Further the absorption spectra confirm to have good absorption in the entire visible region along with a strong absorption in the UV.

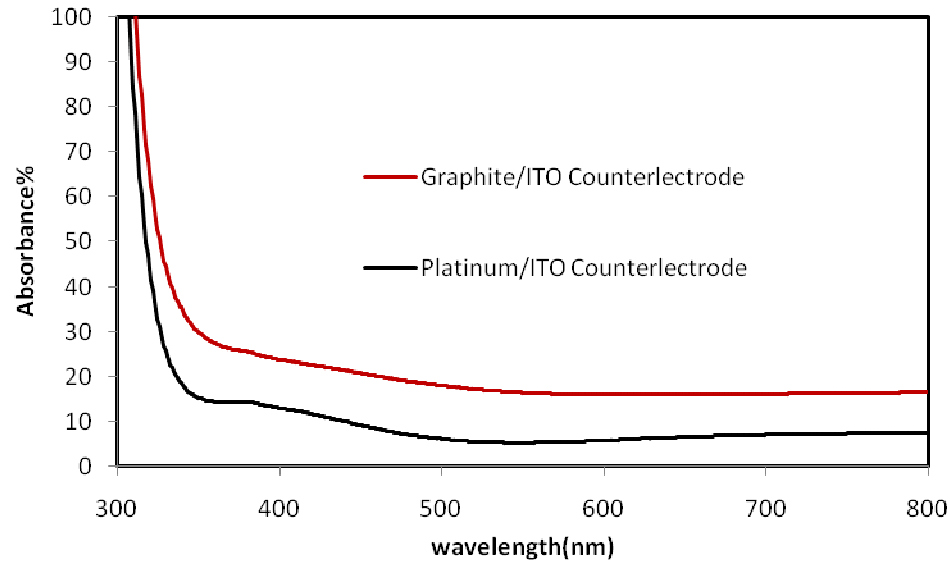


Figure 9 Absorbance spectra of graphite/ITO glass and platinum/ITO glass counter electrode

The optical absorbance spectra of the graphite and platinum electrodes were measured to investigate their potential use for the transparent counter electrodes in DSSC. Figure 9 shows the absorbance spectra of platinum/ITO glass and graphite/ITO glass in the wavelength region 350-800nm. The absorption spectrum of platinum/ITO glass electrode and graphite/ITO glass as a counter electrode was found 7-17% and 20-25% respectively.

3.6 I-V characteristics

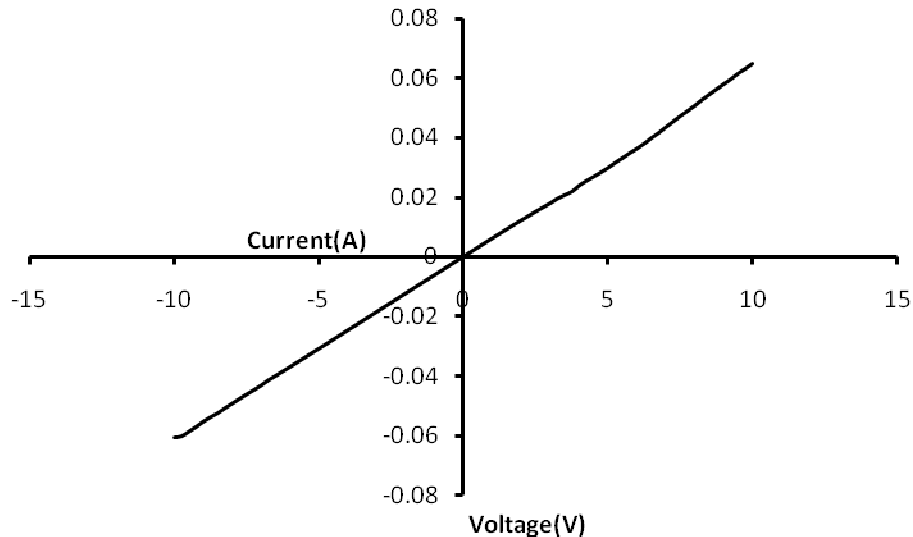


Figure 10 I-V characteristic of ITO film.

The current voltage characteristics of ITO film coated on the glass substrate show the current (I)-voltage (V) graph to have a linear nature as shown in figure 10.

3.7 Open circuit voltage decay

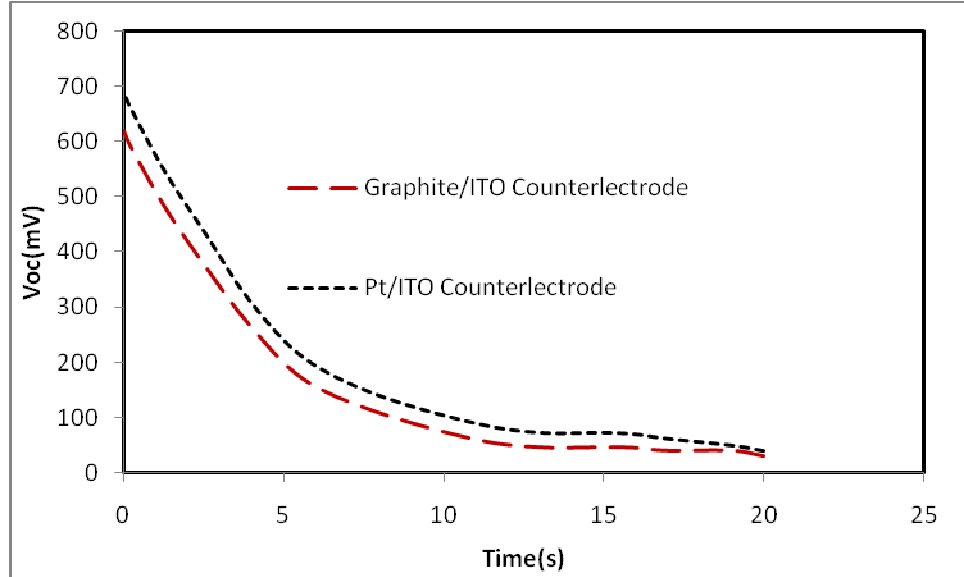


Figure 11 Open circuit voltage decay with time.

The V_{oc} decay with time of two DSSCs for platinum/ITO glass electrode and graphite/ITO counter based electrode as shown in fig.11. The ITO glass under constant illumination, the solar cell reaches a photo-stationary situation. The open circuit voltage may be expressed in the terms of electrons concentration in conduction band.

$$V_{oc} = \frac{kT}{e} \ln \frac{n}{n_0} \quad (2)$$

Here, kT is the thermal energy, e is the positive elementary charge, and n_0 is the electron concentration in the dark, the recombination rate has a major impact on the open-circuit voltage obtained at any light intensity. Information on the properties of the recombination process can be obtained from the correlation V_{oc} in the steady state. The starting point for the V_{oc} decay measurement is the non equilibrium steady state of a cell illuminated at constant intensity I_0 . The illumination is interrupted, and $V_{oc}(t)$ is recorded, while the cell is kept at open circuit. During the decay, n evolves from the initial steady state value to the dark equilibrium with concentration n_0 .

3.8 Performance of DSSC

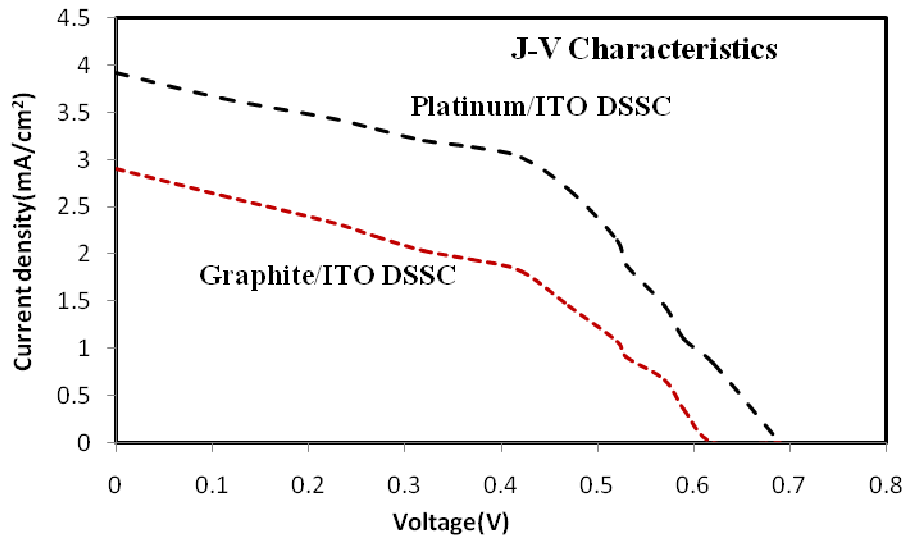


Figure 12 J-V characteristics of DSSCs.

Table1 Performance of graphite and platinum based DSSC

Sample	Voc(mV)	I _{sc} (mA)	FF	Efficiency (%)	J _{sc} (mA/cm ²)
Graphite/ITO DSSC	619.5	2.90	0.503	0.89	2.90
Platinum/ITO DSSC	690.1	3.92	0.603	1.63	3.92

The values of fill factor (FF) and efficiency (η) of DSSC were calculated by following equations.

$$FF = \frac{I_m V_m}{I_{sc} V_{oc}} \quad (3)$$

V_{oc} - open circuit voltage, I_{sc} - short circuit voltage, I_m - max. current and V_m - maximum volatage.

$$\eta = \frac{I_{sc} V_{oc} FF}{P_{in}} \quad (4)$$

Here FF is the fill factor, η is the efficiency and J_{sc} is current density of DSSC. The performances of DSSCs were characterized at $100\text{mW}/\text{cm}^2$ intensity shown in figure 12. The V_{oc} of platinum and graphite based DSSC are obtained 690.1 mV and 619.52mV respectively. The short circuit current is I_{sc} is found 3.92mA and 2.9 mA for platinum/ITO glass and graphite/ITO glass respectively. A mask with a window of $1\text{cm} \times 1\text{cm}$ was also clipped on the TiO_2 side to define the active area of the cell.

The value of FF is 0.60 and 0.50 for platinum and graphite electrodes respectively. The efficiency of platinum/ITO glass and graphite/ITO glass counter-electrode were obtained as 1.63% and 0.89% respectively. The electron transport between the graphite and conducting substrate is low as compared to platinum as counter-electrode and this hinders the overall performance of the DSSCs [23]. However, graphite as alternative material to platinum in DSSCs is a promising

research area. Moreover graphite based DSSC reduces the cost of the devices for commercialization.

4. Conclusions

XRD pattern confirm that TiO_2 photo-anode of DSSC were successfully prepared. Prepared TiO_2 film has a mixture of anatase and rutile phases. The synthesized film is an excellent adhesive with the ITO glass substrate. FESEM confirmed that surface of film is porous in nature. The decay of V_{oc} with time shows a non linear behavior. The V_{oc} of platinum/ITO glass based dye solar cell was obtained to be 690.1mV, but in the case of graphite its value was found to be 619.5mV. The fill factor for platinum and graphite based DSSC were obtained as 0.60 and 0.50 respectively. The efficiency of DSSC for platinum and graphite as counter electrode were 1.63% and 0.89% respectively. Comparison of the efficiency and fill factor of the counter electrodes with different materials measured under similar conditions showed that platinum DSSC have higher efficiency as compared to DSSC with graphite electrode. But, graphite is the most economical material for application as a counter electrode in DSSCs, which needs further research.

Acknowledgement

Authors are also thankful to SAIF/CIL Panjab University, Chandigarh for providing experimental facilities.

REFERENCES

- [1] S. Chappel , Si-Guang Chen, A. Zaban, "TiO₂-Coated Nanoporous SnO₂ Electrodes for Dye-Sensitized Solar Cells", *Langmuir*, **8**, 3336-3342 (2002).
- [2] I. Bedja , P.V. Kamat, X. Hua, A.G. Lappin, S. Hotchandani, "Photosensitization of Nanocrystalline ZnO Films by Bis (2, 2 '-bipyridine)(2, 2 '-bipyridine-4, 4 '-dicarboxylic acid) ruthenium (II)", *Langmuir*, **13**, 2398-2403 (1997).
- [3] K. Keis, "Nanostructured ZnO electrodes for dye-sensitized solar cell applications", *J. Photo-chem. Photobiol Chem.*, **148**, 57-64 (2002).
- [4] O. Carp, C.L. Huisman, A. Reller, "Photoinduced Reactivity of Titanium Dioxide", *Prog. Solid State Chem.*, **323**, 3-177(2004).
- [5] A. Fujishima, T.N. Rao , D.A.J. Tryk, "Titanium Dioxide Photocatalysis", *Photochem. Photobiol.*, **1(1)**, 1-21(2000).
- [6] M.R. Hoffmann, S.T. Martin, D.W. Choi, D.W. Bahnemann, "Environmental Applications of Semiconductor Photocatalysis", *Chem. Rev.* **95**, 69-96 (1995).
- [7] M. Fujihira, Y. Satoh, T. Osa , "Heterogeneous photocatalytic oxidation of aromatic compounds on titanium dioxide", *Nature London*, **293**, 206-208 (1981).
- [8] N. Park, "Light management in dye-sensitized solar cell", Korean, *J. Chem. Eng.*, **27**, 375-384 (2010).
- [9] G. Schlichthrl, S.Y. Huang, J. Sprague, "Band Edge Movement and Recombination Kinetics in Dye-Sensitized Nanocrystalline TiO₂ Solar Cells: A Study by Intensity Modulated Photovoltage Spectroscopy", *J. Phys. Chem. B*, **101**, 8141-8155 (1997).

- [10] A. C. Fisher, L.M. Peter, E.A. Ponomare, A.B. Walker, K.G.U. Wijayantha, "Intensity Dependence of the Back Reaction and Transport of Electrons in Dye-Sensitized Nanocrystalline TiO₂ Solar Cells", *J. Phys. Chem. B*, **104**, 949 (2000).
- [11] S. Sdergren, A. Hagfeldt, J. Olsson, S.E. Lindquist, "Theoretical Models for the Action Spectrum and the Current-Voltage Characteristics of Microporous Semiconductor Films in Photoelectrochemical Cells", *J. Phys. Chem.*, **98**, 5552 (1994).
- [12] N.W. Duffy, L.M. Peter, R.M.G. Rajapakse, K.G.U. Wijayantha, "Investigation of the Kinetics of the Back Reaction of Electrons with Tri-Iodide in Dye-Sensitized Nanocrystalline Photovoltaic Cells", *J. Phys. Chem. B*, **104**, 8916 (2000).
- [13] M. Berginc, U. Opara Krasovec, M. Jankovec, M. Topic, "The effect of temperature on the performance of dye-sensitized solar cells based on a propyl-methyl-imidazolium iodide electrolyte", *Sol. Energy Mater. Sol. Cells*, **91**, 821-828 (2007).
- [14] M. Berginc, U. Opara Krasovec, M. Hocevar, M. Topic, "Performance of dye-sensitized solar cells based on Ionic liquids: Effect of temperature and iodine concentration", *Thin Solid Films*, **516**, 7155-7159(2008).
- [15] A. Singh, D. Mohan, D.S. Ahlawat, Richa, "Performances of spin coated silver doped ZnO photoanode based dye sensitized solar cell", *Processing and Application of Ceramics*, **11**, 213-219 (2017).
- [16] J. Han, H. Kim, D.Y. Kim D, S.M. Jo, S. Jang, "Water-Soluble Polyelectrolyte-Grafted Multiwalled Carbon Nanotube Thin Films for Efficient Counter Electrode of Dye-Sensitized Solar Cells", *ACS Nano*, **4**, 3503-3509 (2010).
- [17] Unique U. Opara Krasovec, M. Berginc, M. Hocevar, M. Topic, "*Solar Energy Materials & Solar Cells*", **93**, 379-381 (2009).
- [18] A. Singh, D. Mohan, D.S. Ahlawat, Richa, "Influence of dye loading time and electrolytes ratio on the performance spin coated ZnO photoanode based dye sensitized solar cells", *Orient J. of Chem.*, **32**, 1049-1054 (2016).
- [19] A.M. Khan, M. A. Shaheer, Y. Bong, "Synthesis and Characterization of Mesostructured Titania-Based Materials through Evaporation-Induced Self-Assembly", *Solar Energy*, **84**, 2195-2201 (2010).
- [20] M. Adachi, Y. Murata, I. Okada, S. Yoshikawa, "Formation of Titania nanotubes and applications for dye-sensitized solar cells", *J. Electrochem. Soc.*, **150**, 488-493(2003).
- [21] C. Longo, M. DePaoli, "Dye-sensitized solar cells: a successful combination of materials", *J. Braz. Chem. Soc.*, **14**, 889-901(2003).
- [22] A. N. Jose, J.T. Juan, D. Pablo, R.P. Javier, R. Diana, I.L., Marta, *Appl. Catal., A Gen.*, **178** (1999) 91.
- [23] I. Chena, Y. Weib, M. Tsabib, F. Tsengb, S. Weic, H. Wua, Chien-KuoHsieha, "High performance dye-sensitized solar cells based on platinum nanoroses counter electrode", *Surface and Coatings Tech.*, **320**, 409-413 (2017).